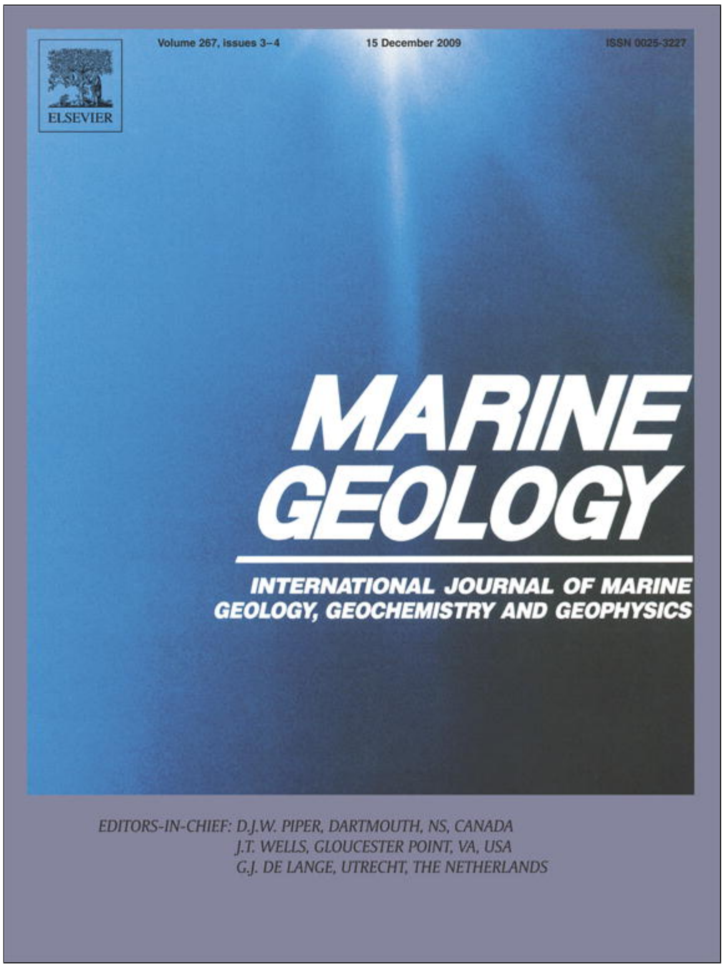
Volume 267, issues 3–4
15 December 2009
ISSN 0025-3227
ELSEVIER
MARINE GEOLOGY
INTERNATIONAL JOURNAL OF MARINE GEOLOGY, GEOCHEMISTRY AND GEOPHYSICS
EDITORS-IN-CHIEF: D.J.W. PIPER, DARTMOUTH, NS, CANADA
J.T. WELLS, GLOUCESTER POINT, VA, USA
G.J. DE LANGE, UTRECHT, THE NETHERLANDS

Marine Geology 267 (2009) 175–190

Contents lists available at ScienceDirect

Marine Geology

journal homepage: www.elsevier.com/locate/margeo

Remote sensing of sand distribution patterns across an insular shelf: Oahu, Hawaii

C.L. Conger [a,*], C.H. Fletcher [b], E.H. Hochberg [c], N. Frazer [b], J.J.B. Rooney [d]

[a] University of Hawai'i at Manoa, School of Ocean and Earth Science, Sea Grant College Program, 2525 Correa Road, Honolulu, Hawai'i 96822, USA
[b] University of Hawai'i at Manoa, School of Ocean and Earth Science, Department of Geology and Geophysics, 1680 East-West Road, Honolulu, Hawai'i 96822, USA
[c] Nova Southeastern University, Oceanographic Center, 8000 North Ocean Drive, Dania Beach, FL 33004, USA
[d] Joint Institute for Marine and Atmospheric Research, University of Hawaii, Pacific Islands Fisheries Science Center, National Marine Fisheries Service, Kewalo Research Facility, 1125-B Ala Moana Blvd., Honolulu, HI 96814, USA

ARTICLE INFO

Article history:
Received 16 April 2009
Received in revised form 30 September 2009
Accepted 6 October 2009
Available online 17 October 2009

Communicated by J.T. Wells

Keywords:
shelf sand
reef
spatial statistics
Hawaii
remote sensing
classification

ABSTRACT

Sandy substrate is important as a resource, habitat, and dynamic region of the bathymetry. We find that sand storage across the insular shelf of Oahu, Hawaii is controlled most strongly by general insular shelf morphology and to a lesser degree by hydrodynamic energy. Shelf sand is predominantly found in water depths less than or crossing the 10 m contour. We use remote sensing to identify and classify 14,037 individual sand deposits in nine study regions. A supervised classification algorithm aggregates these into five classes with 14 subclasses. Almost 63% of all sandy surface area falls into two subclasses of the Channels and Connected Fields class, 1) Major Channels and 2) Unchannelized Drainage. These subclasses connect regions of sediment production to regions of sediment storage on the insular shelf surface. This study is the first to quantitatively analyze and classify shelf sand deposits, in a high volcanic island coral reef setting.

1. Introduction

Sandy marine substrate is an important component of coastal and shelf habitat, a valuable resource for beach renourishment and construction, and a dynamic component of the bathymetry. The shape and form of nearshore sand deposits have a pronounced effect on shoreline stability and constitute a significant portion of Hawaii's coastal geologic framework (Fletcher et al., 2008). However, relatively little is known of shallow insular shelf sand bodies on low-latitude coasts, despite the significance of nearshore sands in managing the coastal environment (Bochicchio et al., 2009). This study aims to characterize meso-scale (10's of square meters to square kilometers) spatial patterns of sand occurrence on the shelf of Oahu, Hawaii (Fig. 1) with a generalized classification system based on spatial statistics.

In contrast to continental locations, where siliclastic sediment is supplied by streams and erosion of coastal sources, the sands of Oahu are primarily carbonate. They are composed of skeletal fragments of marine organisms and accumulate in relatively thin patches, fields, and linear deposits upon narrow insular shelf surrounding the island (Moberly et al., 1965; Harney et al., 2000; Harney and Fletcher, 2003; Hampton et al., 2003; Grossman et al., 2006; Fletcher et al., 2008). Insular shelf sand bodies reflect a balance of factors including production, temporary and permanent storage, and loss (including abrasion, dissolution, bioerosion, and offshore transport; Harney and Fletcher, 2003). A combination of hydrodynamic energy, water quality, biologic productivity, and seafloor topography all control creation, destruction, and storage of carbonate sands. Historical changes in sea-level shape insular shelf morphology through alternating subaerial and marine exposures, and combine with modern coral communities to play key roles in shaping the storage capacity of the insular shelf. Three studies (Moberly et al., 1975; Sea Engineering, 1993; Bochicchio et al., 2009) have cataloged these nearshore sands.

Our study focuses on the sandy substrate extending from the shoreline to an approximate depth of 20 m below sea-level. Both coral and algal growth rates are highest in these depths (Stoddart, 1969) because of water circulation and nutrient availability, wave climate (Grigg and Epp, 1989; Grigg et al., 2002), and available light. Most sediment on the insular shelf is produced by reef builders, reef dwellers, and reef bioeroders, making this zone the primary source of nearshore sands. Only in the last 8500 yr have sea-level rise and shoreline transgression led to the inundation of this portion of the insular shelf (Grigg, 1998) and allowed for modern carbonate accretion (Fletcher and Sherman, 1995; Harney et al., 2000; Grigg et al., 2002; Harney and Fletcher, 2003, Grossman et al., 2006).

* Corresponding author. Tel.: +1 808 587 0049; fax: +1 808 956 3259.
E-mail addresses: conger@hawaii.edu (C.L. Conger), fletcher@soest.hawaii.edu (C.H. Fletcher), eric.hochberg@nova.edu (E.H. Hochberg), neil@soest.hawaii.edu (N. Frazer), John.Rooney@noaa.gov (J.J.B. Rooney).

0025-3227/$ – see front matter © 2009 Elsevier B.V. All rights reserved.
doi:10.1016/j.margeo.2009.10.005

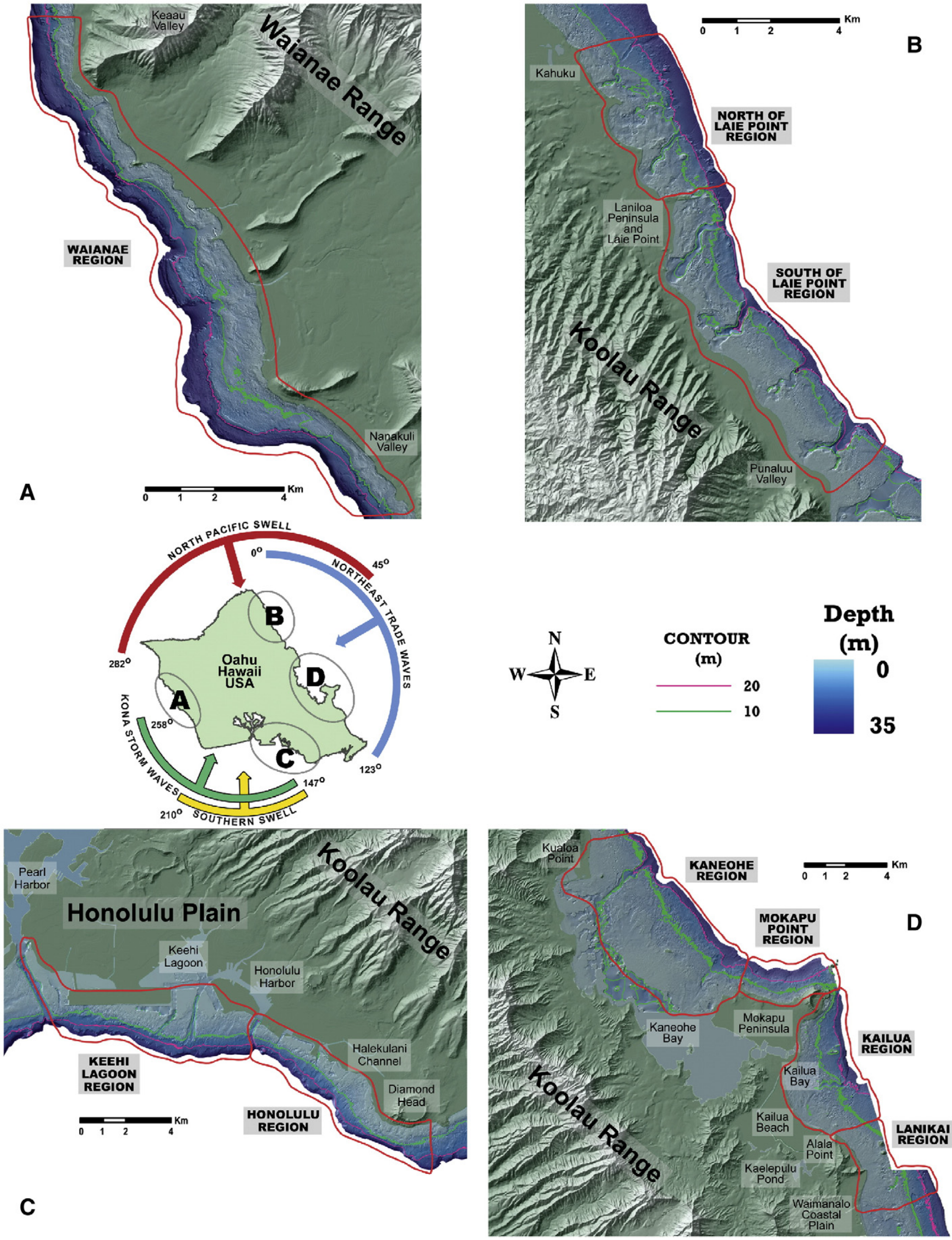

Fig. 1. Bathymetry and topography of Oahu coastal zone, interpolated from SHOALS LIDAR data and USGS DEM. A, B, C, and D show Waianae region; South of Laie Point and North of Laie Point regions; Honolulu and Keehi Lagoon regions; and Lanikai, Kailua, Mokapu Point, and Kaneohe regions respectively.

Most waves reach wave base within the zone 0–20 m and convert their wave energy into shear stress across the sea floor, providing a means for mechanical abrasion of both carbonate framework and direct sediment producers (Storlazzi et al, 2003; Storlazzi et al, 2005). On Oahu, 20 m marks the approximate edge of the nearshore shelf that terminates in a shallow, seaward facing scarp that is part of the Kaneohe Shoreline Complex evident around much of the island (Stearns, 1974; Fletcher and Sherman, 1995). By extension of the Hawaiian eolianite model proposed by Stearns (1970) and modified by Fletcher et al. (2005) where this scarp prevents sand transport upslope by winds during times of lowered sea-level, it may also act as a barrier for shoreward submarine transport except where channelized, similar to the fossil barrier reef off southeast Florida (Finkl, 2004). Importantly, airborne and satellite sensors are capable of accurately imaging the sea floor within this depth range allowing us to prospect for sands via satellite imagery.

2. Regional setting

2.1. Insular shelf

Within the depth range of 0–20 m, morphology of the shelf around Oahu results from carbonate accretion over recent interglacial cycles (for a review, see Fletcher et al., 2008). Most of the shelf in this depth zone is reefal in structure and Marine Isotope Stage (MIS) 7 in origin (Sherman et al., 1999). The front of the shelf is characterized by reefal carbonates from MIS 5a–d, and the shallow landward portion in some areas is covered by eolianites of similar age. Covering the shelf in a patchy distribution around the island and filling in available accommodation space are Holocene reef carbonates (Grigg, 1998; Rooney et al., 2004; Grossman and Fletcher, 2004). The shelf surface has been sculpted through episodes of subaerial weathering and erosion characterizing the last two interglacial cycles. Circumferential to Oahu, the shelf is almost entirely a fringing reef system with a shallow reef flat or a ramped reef face. Exceptions include Kaneohe Bay and possibly Keehi Lagoon, both of which are classified as lagoons with barrier reefs, or reefs intermediate between barrier and fringing morphologies (Guilcher, 1988).

2.2. Wave climate

Wave energy impacts accommodation space and mechanical abrasion on the insular shelf and reef, as well as impacting coastline stability and nearshore submarine sand transport. Bodge and Sullivan (1999) described four main components of Hawaii's regional wave climate, as illustrated in Fig. 1. In the northwest Pacific, high-energy waves are created by winter storms with prolonged high winds directed at the northwestern shores of Hawaii. These waves are incident to shorelines facing from WNW to NNE with typical heights of 1.5–4.5 m and periods of 12–20 s, and extreme heights measured to 15 m. In the south Pacific, high winter (northern hemisphere summer) waves are created between April and October. These south Pacific waves typically have deep-water heights of 0.3–1.8 m and periods of 12–20 s. Infrequent Kona storms produce moderately high-energy waves (around 9% of the year) that approach from the south and west with heights of 3–4.5 m and periods of 6–10 s. Trade wind waves, the most consistent year-round wave type, have moderate energy and approach from the northeast quadrant ~75% of the year, for 90% of the summer months and 55–65% of the winter months (Grigg, 1998). Trade wind waves have heights of 1.2–3 m and periods of 4–10 s. In addition to these four main types of waves, there are also the infrequent but highly destructive hurricane waves that impact nearshore reefs (Grigg, 1998).

3. Methods/materials

The first step in improving understanding of spatial distribution is analyzing the two-dimensional meso-scale (10's of square meters to square kilometers) surface characteristics of insular shelf sands. Spatial analysis is useful for identifying surface characteristics associated with insular shelf morphologies and is helpful for inferring origin and history. The caveats for spatial analysis are that it fails to incorporate sand thickness, temporal variability, and sediment composition properties.

3.1. Study regions

Nine Oahu study regions are defined using available QuickBird Satellite© images. Study sites are chosen based on quality of available scenes, diversity of the nearshore region, and representation of distinct types of shorelines. These are spread around the perimeter of Oahu, and cover approximately 39% of the total length of shoreline and 125 km^2 of reef. The regions are detailed in Table 1.

3.2. Remotely sensed images

Four images were used in this study to characterize sediment distribution patterns in nearshore waters of Oahu. QuickBird Satellite scenes for this purpose were provided by DigitalGlobe, Inc., at http://www.digitalglobe.com. These are georectified, multi-channel (blue 450–520 nm, green 520–600 nm, red 630–690 nm, and NIR 760–900 nm), TIFF images of Oahu, Hawaii, with 2.4 m pixel resolution. Images for regions are identified in Table 1.

3.3. LIDAR bathymetry

SHOALS (Scanning Hydrographic Operational Airborne LIDAR Survey) LIDAR (Light Detection and Ranging) was acquired and processed by the U.S. Army Corps of Engineers (USACE). LIDAR data for regions is identified in Table 1. LIDAR coverage for the island of Oahu is both complete and dense, with an average nearest distance between points of ~2.8 m. LIDAR points for each site (±5 cm vertical resolution) were interpolated using the Natural Neighbors technique in ArcGIS, and rasterized to a pixel size of 2.4 m. Fig. 1 is a mosaic of the interpolated bathymetry, shaded for the depth range from 0 to 35 m below mean sea-level for all study sites.

3.4. Image processing

Following the method in Conger et al. (2006), we decorrelated both blue and green bands from depth. This procedure coregisters bathymetry and satellite datasets, creating band pairs where each pixel has a reflectance value and a known depth value. The deep-water reflectance of each band is subtracted from each pixel's reflectance value. All subaerial regions, surface disturbances, highly turbid waters, and LIDAR abnormalities are removed. An *ln*-transform of the reflectance data approximates the exponential attenuation of light through the water column (Lyzenga, 1978). This simplifies the relationship between light attenuation and changes in water depth to a linear, highly correlated data distribution. Sample pixels are selected across the 0 to 20 m depth range from a single substrate type to minimize variance from reflector types (Mumby et al., 1998). Carbonate sands are used for this because of their easy identification and presence at most depths. These sample pixels are used to model light attenuation with depth. By relating the variability in each band's intensity values to water depth a Principal Component Analysis (PCA) can be used to remove the correlation between depth and light attenuation. A coordinate transformation is applied to an entire band pair (Rencher, 2002). Output from this band pair rotation is a new color band where individual substrates no longer become darker as the water column becomes deeper. Fig. 2A shows the rotated blue color band for a section of Kailua Bay reef used to develop and test this methodology. Data and results from Isoun et al. (2003) were used for comparison.

Table 1
Study regions.

Region	Shelf description	Wave climate	Coastal setting	Remote sensing
Waianae	<0.5 km–>1 km wide Ramped shelf face Numerous paleo-channels	North Pacific swell Kona storms Hurricanes South Pacific swell	Arid climate Broad coastal plain Modern beach	Digital Globe 101001000173E702 USACE LIDAR
North of Laie Point	Narrow and shallow fringing shelf Ramped shelf face Eolianite islets	Trade wind waves North Pacific swell	Wet climate Narrow coastal plain Modern beach	Digital Globe 1010010002B85A01 USACE LIDAR
South of Laie Point	Wide and shallow fringing shelf Numerous paleo-channels	Trade wind waves North Pacific swell	Wet climate Narrow coastal plain Modern beach	Digital Globe 1010010002B85A01 USACE LIDAR
Kaneohe Bay	Shallow shelf Ramped shelf face Lagoon not included	Trade wind waves North Pacific swell	Seaward of the coastline Does not include lagoon or beaches	Digital Globe 03MAR13205953 USACE LIDAR
Mokapu Peninsula	Ramped shelf face Volcanic islet	Trade wind waves North Pacific swell	Coastal plain and post-erosional volcanics Modern beach	Digital Globe 03MAR13205953 USACE LIDAR
Kailua	Ramped shelf face Volcanic and carbonate islets Paleo-channels	Trade wind waves North Pacific swell	Wetland Beach ridge strand plain Modern beach	Digital Globe 03MAR13205953 USGS LIDAR
Lanikai	Wide and shallow fringing shelf Paleo-channels	Trade wind waves North Pacific swell	Beach ridge strand plain Modern beach Basalt headlands	Digital Globe 03MAR13205953 USACE LIDAR
Honolulu	Wide and moderately shallow fringing shelf Paleo and dredged channels	Kona storms Hurricanes South Pacific swell	Coastal plain Post-erosional volcano Filled wetlands	Digital Globe 1010010002D75F04 USACE LIDAR
Keehi Lagoon	Wide and shallow shelf Paleo and dredged channels	Kona storms Hurricanes South Pacific swell	Seaward of lagoon Filled land and island Modern beach	Digital Globe 1010010002D75F04 USACE LIDAR

3.5. Substrate identification

Identification techniques include classification algorithms, band density slices, and analyst selection. The confounding effects of the water column have made marine substrate classification based on reflectance, across large regions, marginally successful at best, with no single technique capable of routinely solving the problem. We use a combination of several techniques to reduce the effects of variation in water column properties, atmospheric properties, and sea-surface state.

Simple classifier algorithms are used to segregate processed images into two categories, *Sand* and *Other Than Sand*. A minimum distance classifier (Rencher, 2002) is used on most image segments. Accuracy for classification runs is assessed by two methods: test statistics (Rencher, 2002) and analyst interpretation. Test statistics account for the number of correctly and incorrectly identified pixels, but are often insufficient for our purposes. We focus on analyst interpretation, which permits choosing the best classification based on its spatial accuracy. Fig. 2B shows the classified image for a section of Kailua Bay.

In addition to the classification algorithms, application of a band threshold tool is used. The analyst can identify a specific intensity level in a single color band that separates carbonate sands (which tend to be very bright) from all other, and darker, substrate types. An advantage of adjusting the intensity level, or threshold, for the Sand/Other Than Sand boundary is the accommodation of variable water quality characteristics that otherwise introduce error. Increased turbidity by non-carbonate suspended material usually darkens a scene, and carbonate sediment held in suspension usually brightens a scene. A combination of test statistics and analyst interpretation is used to verify successful identification.

Additionally, some sections of each scene are defined by the analyst using simple digitization. These locations are readily identifiable by an analyst. For instance, steep slopes typically create marginal errors with image processing. In these cases digitizing improves border definition

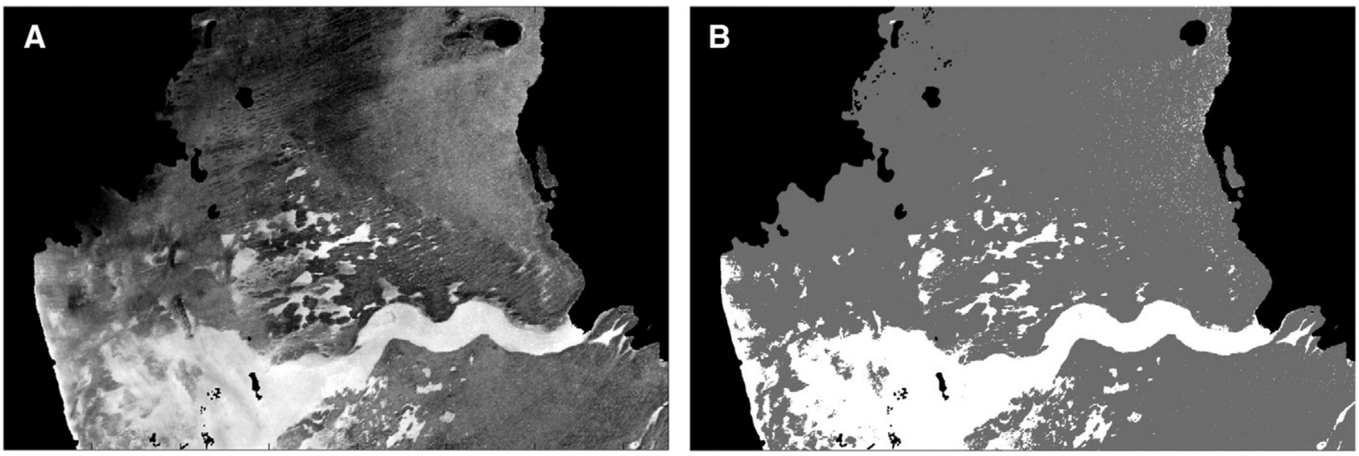

Fig. 2. A section of Kailua region is used as an example of the classification process. A mask, indicated by black pixels, is applied to the imagery. (A) Rotated blue color band, decorrelated from water depth. (B) Classified image, identifying sand (white) and everything other than sand (gray).

on adjacent sand deposits. Some locations do not have usable imagery or LIDAR data, but have been classified on the basis of field observations. The final result, from combined techniques, is a sand identification image of the entire study area, as seen in Fig. 3.

Normal image processing assumes both vertical and horizontal homogeneity within the water column. As this is not usually the case, an image needs to be processed in several sections reflecting different water quality areas. Selection of the identification technique that is appropriate for each section is a function of water quality and varies across each study region. Substrate identification methods are then performed on each individual section. There may be regions in an image that are unusable, or must be identified by the analyst, as are the cases where LIDAR data are not present or are incorrect, and where the imagery is obscured by clouds or sea-surface clutter. This process requires optically shallow waters, meaning that water must be sufficiently clear and shallow for the sensor to record an image of the bottom. This is important because the red and near infrared bands provide very little water penetration, and high turbidity can mask the bottom in the blue and green bands as well. Also, distinction between Sand and Other Than Sand can be subjective, with the definition of

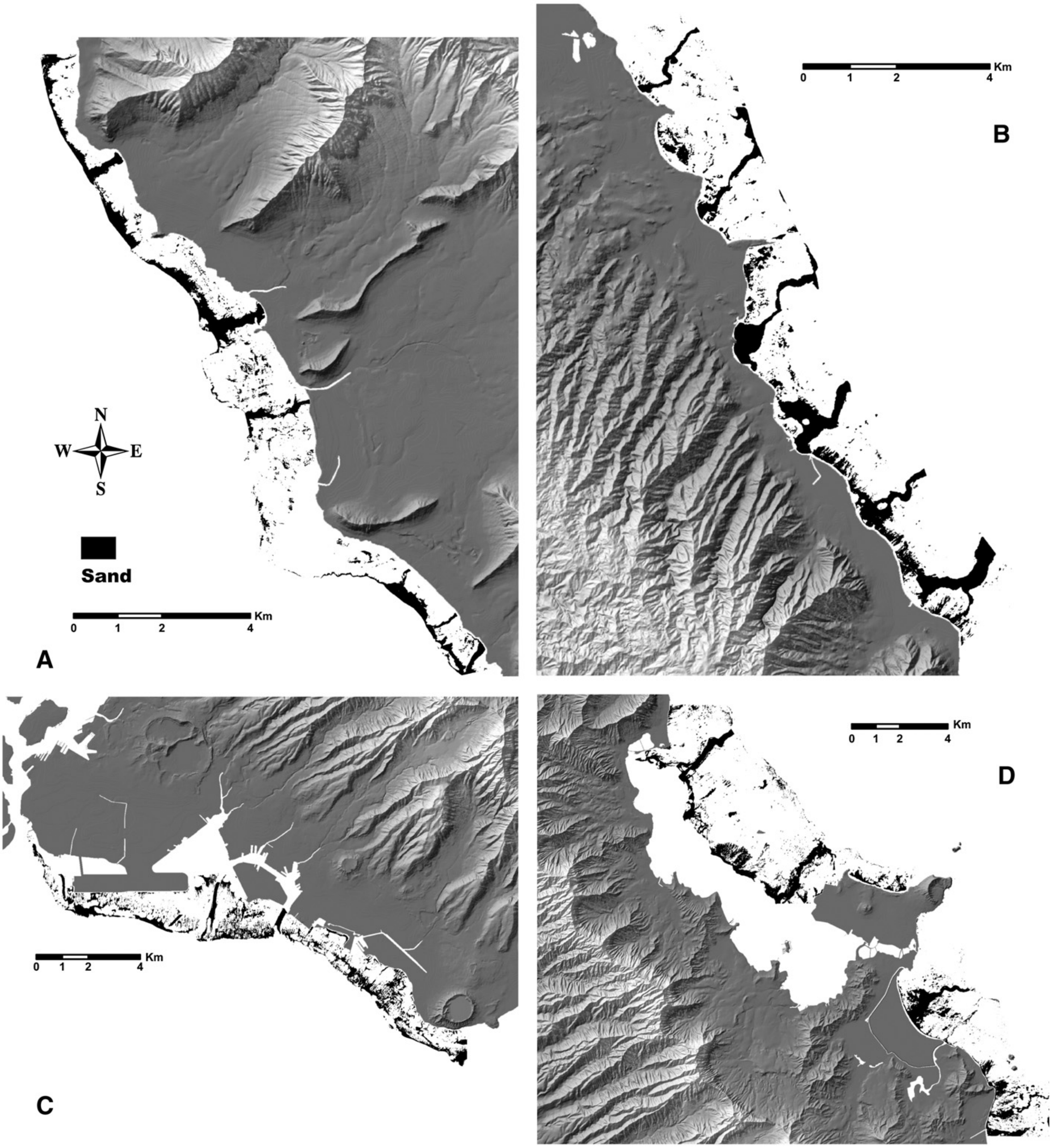

Fig. 3. All classified sands are displayed alongside a topographic map of Oahu. Sections A, B, C, and D correspond to the same sections in Fig. 1.

these two categories coming from within a continuum of substrate variation (as sand grades into hard substrate, rubble, algal meadows, *etc.*) being an analyst decision. This distinction and the subsequent selection of training classes define how and what we identify as sandy substrate for our analysis. All supervised classification techniques require analyst determinations in the beginning, by choosing training and test pixels from field data and image analysis. Our method allows for additional tuning by comparing the spatial qualities of the results to the image data, and by combining techniques to maximize effectiveness. These decisions are made according to the water quality, bathymetry, substrate type, and results for each section.

3.6. Shape analysis

The classified image is segmented, using ENVI software, giving all of an individual sand deposit's pixels the same identification number. We identify a total of 14,037 sand deposits, with a minimum of five connected pixels. We use Matlab to calculate a set of shape measurements for each sand deposit. We use six measurements, they are: area, orientation, eccentricity, form factor, roundness, and solidity. Table 2 lists these measurements, their formulas, and a short description of their physical meaning.

3.7. Image segregation

A supervised classification algorithm is used to identify five discrete classes of sand deposits. The five training classes are described in Table 3. They are: 1. *Channels and Connected Fields*, 2. *Complex Fields and Very Large Depressions*, 3. *Large Depressions and Fields*, 4. *Linear Deposits*, and 5. *Small Depressions and Simple Fields*.

The five classes of sand deposits are split into three depth groups, providing insight into sand storage variability. These groups are: 0–10 m, 10–20 m, and those deposits that straddle the 10 m contour. The 10 m contour approximates the boundary of two insular shelf sub-environments: 1) shallow shelf limited by wave-generated shear forces where bathymetry largely reflects antecedent karst morphology, and 2) deeper shelf where wave forces are less significant and the bathymetry is more likely to reflect modern carbonate accretion related to reef growth. Also, shear stress from wave-generated and tidal currents determines sediment transport (Cacchione and Tate, 1998; Storlazzi et al., 2004) across the insular shelf. Shear stresses from waves are a function of wave amplitude and water depth. The 10 m contour is characterized by intermediate or transitional depths where the substrate is some combination of karst morphology modified by modern reef growth. Comparing these depth groups highlights the ability of the insular shelf to store sands in variable hydrodynamic conditions. Sand deposits within sub-environment crossing 10 m are of special interest as they contain the majority of surface area among sand deposits.

4. Results

The study area comprises nine regions, totaling approximately 125 km^2 of reef. Total surface area of identified sand deposits is about 25 km^2 or ~20% of the total insular shelf area. Channels and Connected Fields account for the majority (64%) of all sand deposit surface area, and Complex Fields and Very Large Depressions account for 18%. Just over 72% of all sand deposit surface area straddles the 10 m contour line, and 24% is <10 m. Combined sands crossing or shallower than 10 m represent more than 96% of all sand deposit surface area. When deposit classes are distinguished by depth range, Channels and Connected Fields that straddle the 10 m contour account for 63%, Complex Fields and Very Large Depressions <10 m account for 10%, and Complex Fields and Very Large Depressions that cross the 10 m contour account for 7%. Together, these three subgroups total 80% of all surface area for sand deposits.

Table 2
Shape measurement equations and descriptions.

Area	Pixel count $\times (2.4\ \mathrm{m})^2$	Converts pixel count to square meters
Orientation	Relative to histogram peak orientation	Each study region is adjusted so that a histogram peak of all sand deposits is at zero degrees, and all orientations are within ±90°, normalizing for all regions.
Form factor	$\frac{4 \times Area \times \pi}{(Perimeter)^2}$	Degree of rugosity around the perimeter of each sand deposit, when compared to an equal area circle's perimeter.
Roundness	$\frac{4 \times Area}{\pi \times (Major\ axis)^2}$	Comparing sand deposit area to a circle with radius equal to the deposit's major axis.
Solidity	$\frac{Area}{Convex\ area}$	How full a sand deposit is, compared to a smooth shape whose perimeter intersects the outer points of the sand deposit's perimeter.
Eccentricity	$\sqrt{1-\left(\frac{Minor\ axis^2}{Major\ axis^2}\right)}$	Measures elongation of a sand deposit within the range from a circle (0) to a line (1).

Study region boundaries are determined by physical variation as described in Section 3.1, not size constraints. Total surface coverage is highly dependent on the aerial extent of the region, so percent regional sand coverage, a normalized measure, is used to compare regions without the influence of aerial extent. Fig. 4 illustrates differences between total surface coverage and percent sand coverage by region. Regions containing the greatest absolute sand cover are Kaneohe and South of Laie Point (Fig. 4A). However, percent regional sand cover is greatest in Honolulu and Keehi Lagoon regions (Fig. 4B).

Fig. 5 displays a glyph plot for each region. Glyph plots are star shaped plots that assign spokes to each of five shape measurements for each region. The shape measure called orientation is not included because in an island setting shorelines are oriented to all points on a compass. Longer spokes indicate a higher value relative to the other

Table 3
Sand deposit class descriptions.

Classes	Descriptions
Channels and Connected Fields	Paleo-stream channels typically starting at or near the shoreline or a nearshore sand field and extending to an offshore sand field. These are highly complex, very elongate, non-rounded, open structures that cover large surface areas.
Complex Fields and Very Large Depressions	Large sand fields made complex by their size, long perimeter, great number of outcrops, and rugged interaction with fringing substrate. Complex Fields and Very Large Depressions are significantly more rounded and solid than Channels and Connected Fields. Large groups of interconnected depressions are also included in this class.
Large Depressions and Fields	Large openings in the insular shelf with steep sides, and fields smaller, less complex, and more solid than Complex Fields and Very Large Depressions. These depressions likely result from solution basins and blue holes filling with available sands. Though original depressions were formed as dolines, uvalas, and possibly poljes during subaerial exposure, modern shape and orientation are likely due to coalescing and reshaping of depressions by modern hydrographic conditions. Medium sized fields also fit into this class.
Linear Deposits	Sands in a linear and fairly simple shape. These fill in linear depressions in the insular shelf, usually in spur and groove, ridge and runnel, or furrow morphologies. They are also elongate bands extended by current and wave energies across the insular shelf.
Small Depressions and Simple Fields	Depressions are individual dolines or small uvalas. Fields are very simple fields, often filling in minor swales or undulations on the insular shelf. Similar to those in Large Depressions and Fields, except small areas with much simpler shapes. The average size limit is around 140 m^2, so they are only small by relative terms.

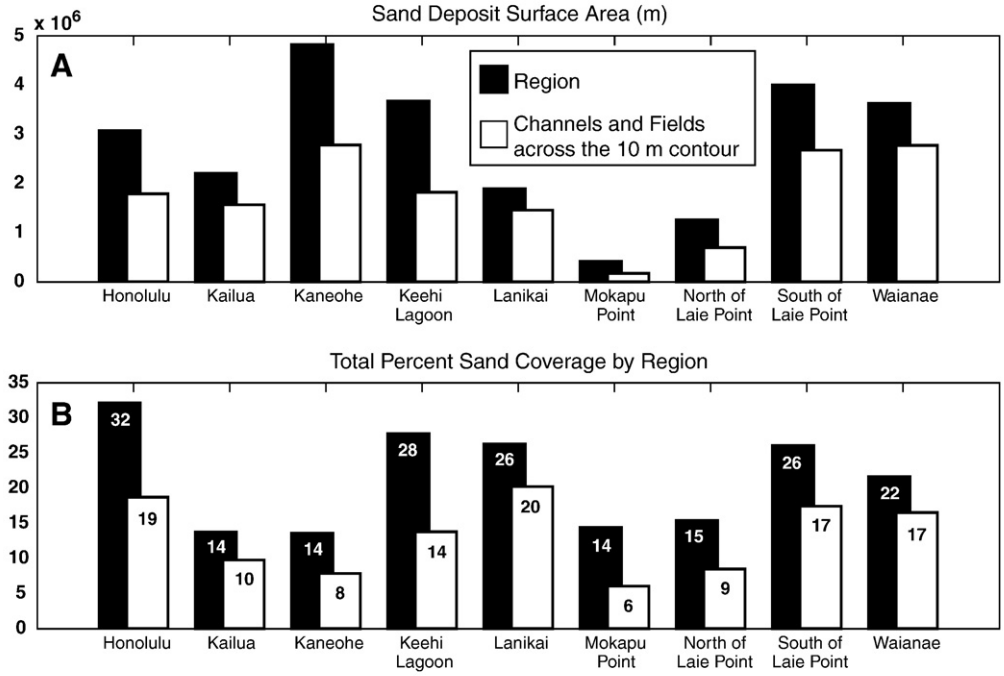

Fig. 4. Two bar plots: A) total sand area by region, and B) total percent sand coverage in each region, normalized by surface area for each region. Overlapping each region's bar is a shorter bar representing the surface coverage for the channels and connected fields crossing the 10 m contour, which accounts for a majority of sand deposit surface area.

regions. An example glyph is provided, with the measurements represented by each spoke labeled. Percent regional sand coverage is used for area. Each glyph displays mean values for eccentricity, roundness, form factor, and solidity for each region. Two areas of the glyph are shaded in the example to illustrate one way to interpret these plots. Complexity indicates a high degree of variability in the shape of the sand deposit. Elongation and circularity indicate generalized geometries of sand deposits.

Dividing sand deposits into classes is an informational tool for defining patterns within the data and mapping out variation between regions. Quantifying the validity for five classes is possible by computing User's accuracy (Rencher, 2002) from an error matrix (Table 4), by calculating the percent of objects identified as a certain class that actually belong to that class. Accuracies are above 90% for all classes except Channels and Connected Fields. The lower User's accuracy results from identifying some deposits from other classes, but this does not significantly change the accuracy of the total surface area classified. User's accuracy is most important because it quantifies the reliability of the classification results. High User's Accuracies imply high confidence in results.

Table 5 lists shape measurement means and standard deviations for each deposit class. Included in the table are bitmap image examples for each class, helpful in understanding actual sand deposits that are associated with specific shape measurement statistics. Glyphs created from the values listed, and short descriptions for each class are included to clarify differences. Also included are small images of sand deposits in each of 14 subclasses. These subclasses are identified by geologic analysis. Variability is represented by one standard deviation about the mean value. Areas have large standard deviation because the surface areas for specific shapes can vary greatly. This does not mean that area measurements are inaccurate; rather they are highly variable within each class and have a wide range of values.

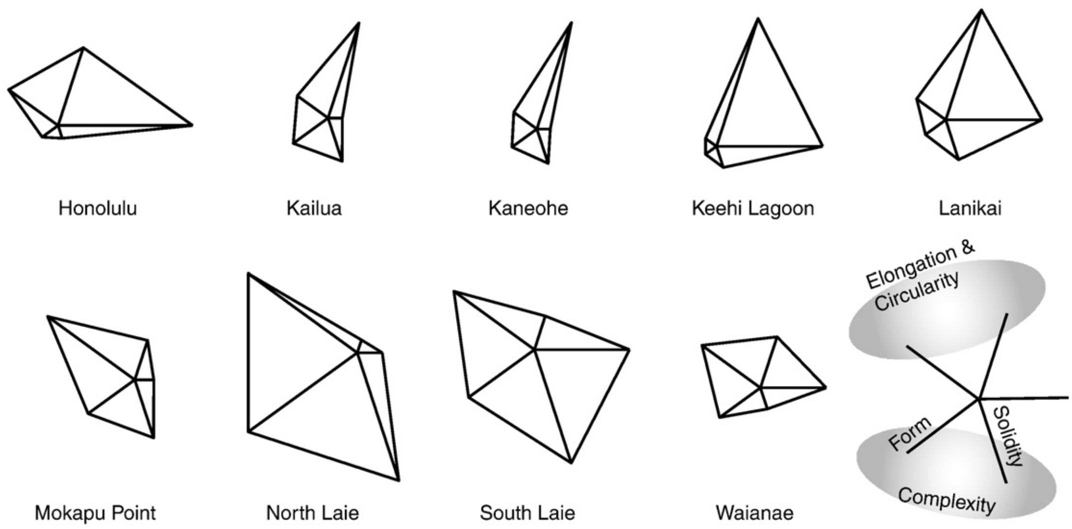

Fig. 5. Glyph plots displaying mean sand deposit shape measurements for the nine regions with arms for percent regional area, eccentricity, roundness, form factor, and solidity. Example glyph is included.

Table 4
User's and producer's accuracies for training classes.

	Channels and Connected Fields	Complex Fields and Very Large Depressions	Large Depressions and Fields	Linear Deposits	Small Depressions and Simple Fields	User's accuracy (%)
Channels and Connected Fields	15	3	3	0	0	71.43
Complex Fields and Very Large Depressions	0	20	1	0	0	95.24
Large Depressions and Fields	0	2	20	0	0	90.91
Linear Deposits	0	0	0	25	0	100
Small Depressions and Simple Fields	0	0	1	0	15	93.75
Producer's accuracy (%)	100	80	80	100	100	

Table 5

Class	Example	Glyph	Description	Area (m²)	Eccentric	Roundness	Form Factor	Solidity
Channels and Connected Fields	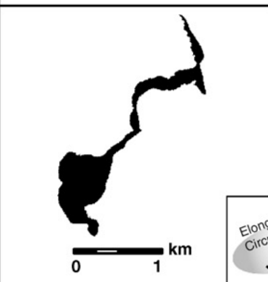	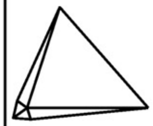	Often long, narrow, and winding with complex borders, complicated shapes, and low solidity values.	165,574 ± 369,520	0.945 ± 0.060	0.128 ± 0.048	0.091 ± 0.048	0.422 ± 0.101
Complex Fields and Very Large Depressions	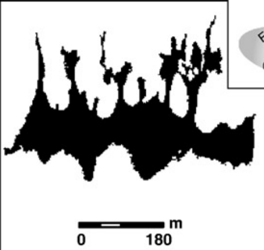		High surface areas with complex open shapes and low solidity values with slightly less elongation and more rounded than channels and connected fieldness.	42,968 ± 112,802	0.851 ± 0.102	0.269 ± 0.105	0.052 ± 0.024	0.475 ± 0.075
Large Depressions and Fields	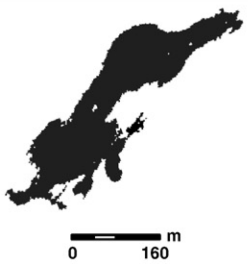		Moderate surface areas, circular to elliptical shapes with moderately complex borders and medium solidity values. 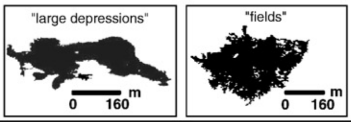	1955 ± 6612	0.785 ± 0.167	0.303 ± 0.128	0.259 ± 0.177	0.549 ± 0.095
Linear Deposits			Lowest surface areas, very linear with eccentricity values close to a line (1.00), very non-circular shapes with simple borders and higher than average solidity values.	50 ± 83	0.975 ± 0.012	0.148 ± 0.050	0.381 ± 0.172	0.686 ± 0.139
Small Depressions and Simple Fields	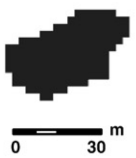	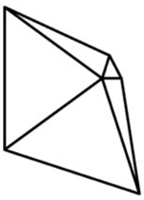	Circular to elliptical simple shapes with smooth borders and very high solidity values. 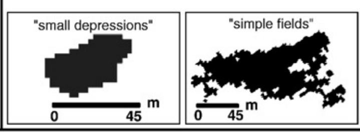	138 ± 53	0.821 ± 0.127	0.417 ± 0.153	1.017 ± 0.536	0.834 ± 0.126

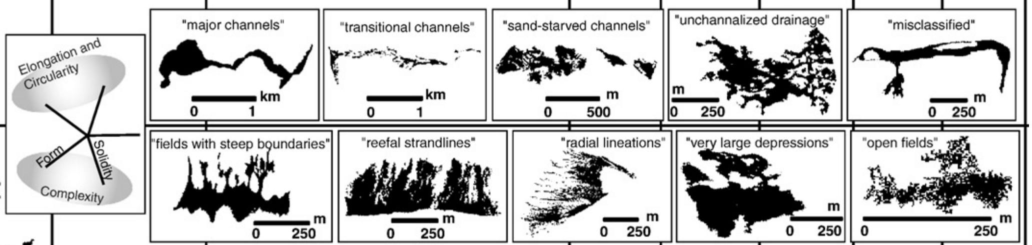

The total population is segregated into five sand deposit classes, in italics, each containing numerous individual sand deposits: *Channels and Connected Fields* (97), *Complex Fields and Very Large Depressions* (103), *Large Depressions and Fields* (1282), *Linear Deposits* (1618), and *Small Depressions and Simple Fields* (10,937).

The five sand deposit classes are each defined by unique assemblages of quantifiable shape measurements, as seen in Table 5. Within each class there are identifiable subclasses, defined using geologic analysis. Final sand deposit class structure is as follows:

1. Channels and Connected Fields
   a. Major Channels
   b. Transitional Channels
   c. Sand-Starved Channels
   d. Unchannelized Drainage
   e. Misclassified Deposits
2. Complex Fields and Very Large Depressions
   a. Fields with Steep Boundaries
   b. Reefal Strandlines
   c. Radial Lineations
   d. Very Large Depressions
   e. Open Fields
3. Large Depressions and Fields
   a. Large Depressions
   b. Fields
4. Linear Deposits
5. Small Depressions and Simple Fields
   a. Small Depressions
   b. Simple Fields

Channels and Connected Fields account for more than 64% of total sand surface area while comprising less than 1% of individual sand deposits. High mean eccentricity (0.945) and low mean roundness (0.128) combined with low mean values for both form factor (0.091) and solidity (0.422) depict elongate, narrow, moderately winding shapes with complex borders. The glyph for Channels and Connected Fields highlights these distinctions. With respect to shape measurements, the glyph is almost opposite that of Small Depressions and Simple Fields. When considering the physical parameters of Channels and Connected Fields, as large sediment conduits across the insular shelf, they contrast obviously with small, isolated deposits. Fig. 6 shows all deposits in Channels and Connected Fields within the study area.

Five common subclasses of channels are identified: 1) Major Channels, 2) Transitional Channels, 3) Sand-Starved Channels, 4) Unchannelized Drainage, and 5) Misclassified Deposits. These are shown in Table 5.

Complex Fields and Very Large Depressions sand deposit class accounts for 18% of the total sand surface area. Almost 17% of the total sand coverage is from Complex Fields in Very Large Depressions in <10 m depth and crossing the 10 m contour, while barely 1% is found in >10 m depth. This does not, however account for all surface sands that are stored in complex fields, as a large portion of nearshore and offshore sand fields are attached to sand channels and classified as Channels and Connected Fields. Moderate mean eccentricity (0.851) and roundness (0.269) describe shapes that are neither round or elongate. Very low mean form factor (0.052) and below average mean solidity (0.422) implies a highly complex boundary to the shape. The glyph plot shows similarity between Complex Fields and Very Large Depressions and Large Depressions and Fields. Though similar, Complex Fields and Very Large Depressions is noticeably more elongate and complex, a result of larger fields and more linked depressions creating complex individual sand deposits. Orientations for this class are bimodal with peaks that are both shore-normal and shore-parallel.

There are, including those fields connected to channels, five main subclasses within Complex Fields and Very Large Depressions: 1) Fields with Steep Boundaries, 2) Reefal Strandlines, 3) Radial Lineations, 4) Very Large Depressions, and 5) Open Fields.

Several key features exist that distinguish this Large Depressions and Fields from other sand deposit classes, including deposit size. Large Depressions and Fields contribute 10% of the total sand surface area. Overall deposit, simpler bathymetric lows, and many more single Large Depressions rather than collections of interconnected depressions, account for lower complexity values. Many of these features are more rounded or elliptical as well as less complex than Complex Fields and Very Large Depressions, they tend to generate higher solidity (0.549) and roundness (0.303) values, with lower form factor (0.259) and eccentricity (0.785) values. This class (10% of total surface coverage) is predominately located in the 0–10 m depth (7% of total surface coverage).

Linear Deposits account for a very small percentage (under 2 %) of the overall sand surface area. They are located throughout the study area with over 75% in the 0–10 m depth. They are very elongate and simple sand deposits. This class has eccentricity values (mean of 0.975) almost equal to a line (1.00); and mean roundness (0.148), mean form factor (0.381), and mean solidity (0.686) values that indicate simple, continuous features with smooth borders.

Small Depressions and Simple Fields account for the majority of individual sand deposits, with almost 78% of those identified in this study, though they only contribute 6% of the total sand surface area. Shape measurements for this class are similar to Large Depressions and Fields, though they reflect the simpler (mean form factor of 1.017), rounder (mean roundness of 0.417 and mean eccentricity of 0.821), and more solid (mean solidity of 0.834) characteristics of these smaller and more cleanly outlined deposits.

These sand deposits are ubiquitous across the depth controlled sub-environments, though most (68% of sand deposits and 75% of surface coverage for this class) are in the sub-environment <10 m depth. Only 2% of these deposits are in the sub-environment crossing 10 m. Few intersect the 10 m contour with radii averaging just less than 5 m. This class is slightly more elongate than the larger depressions.

Fig. 7 contains bar plots of percent regional sand coverage for each class. The sum of all sand deposit classes is depicted in the All Regions plot showing sand distribution pattern for the entire island-wide study. Honolulu region's class distribution pattern is the closest to that of the entire study area, while several regions (i.e. Lanikai, Mokapu Point, and North of Laie Point) have unique class distributions.

Honolulu region and Keehi Lagoon region have the highest percent regional sand coverage at 32% and 28% respectively.

5. Discussion

We analyze the occurrence of five sand deposit classes in the three sub-environments and the total study area of Oahu. Discussion begins with a description of findings for the entire study area then narrows to a discussion of insular shelf environments.

5.1. Sand deposits

Total sand deposit population statistics for the 14,037 sand bodies identified are indicative of Oahu's sand distribution patterns and to some degree its insular shelf morphology. Each of these is a continuous sand body on the reef surface with a minimum size of five pixels, or 28.8 m^2. Most are located in low-lying sections of the bathymetry, produced by subaerial exposure of the fossil reef and modern reef growth. The degree of influence these two processes exert on insular shelf morphology is largely controlled by depth of water (including past sea-level lowerings) and wave climate.

5.1.1. Channels and Connected Fields

Major Channels are easily identified through bathymetry or an image of the insular shelf and are accurately identified by the

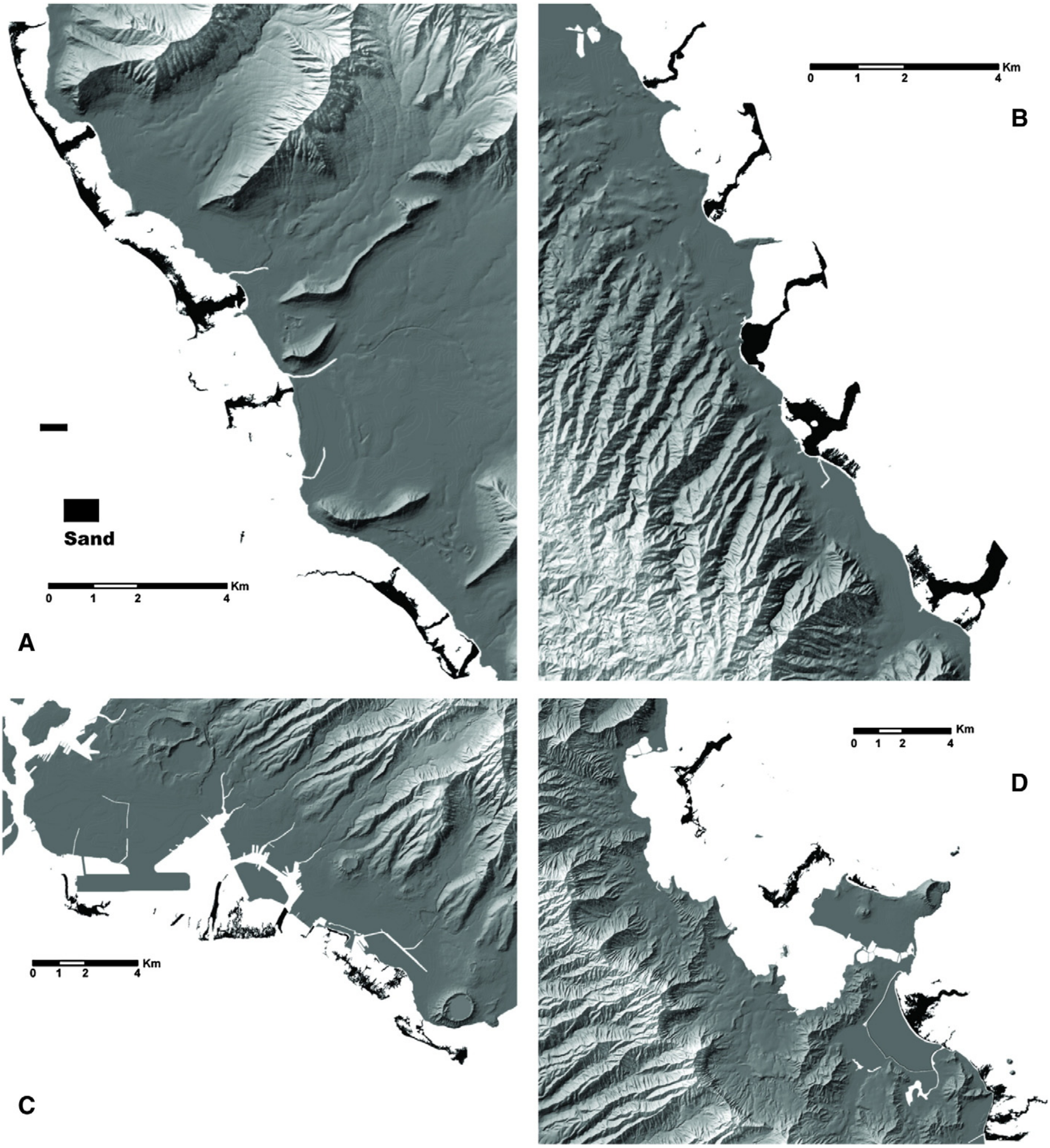

Fig. 6. All Channels and Connected Fields class are displayed alongside a topographic map of Oahu. Sections A, B, C, and D correspond to the same sections in Figs. 1 and 3.

supervised classification. When filled with sand, these units almost always connect to both nearshore and offshore sand fields, acting as conduits for sand movement in onshore and offshore directions.

Major Channels are likely the result of superimposed streams that incised fossil reef during sea-level low-stands. In every case, channel axes are aligned with or in close proximity to their respective modern drainage systems in the adjoining watershed. These sand deposits are typically shore-normal in orientation. Exceptions exist when several stream channels feed into a single sand deposit. All sand deposits in this class cross the 10 m contour. When combined with deposits in the subclass Unchannelized Drainage (also in sub-environment crossing 10 m), they account for almost 63% of total sand coverage and almost all of Channels and Connected Fields' sand coverage.

Two subclasses Transitional Channels and Sand-Starved Channels both lack connectivity between nearshore and offshore sand fields. Limited number of examples on the reef indicates that it is rare for a channel to be filled by modern growth (Purdy, 1974). Major Channels develop from broad superimposed paleo-streams, as evidenced by Grossman and Fletcher (2004) who drilled the walls of a paleo-channel in Kailua Bay. They found that though reef growth is

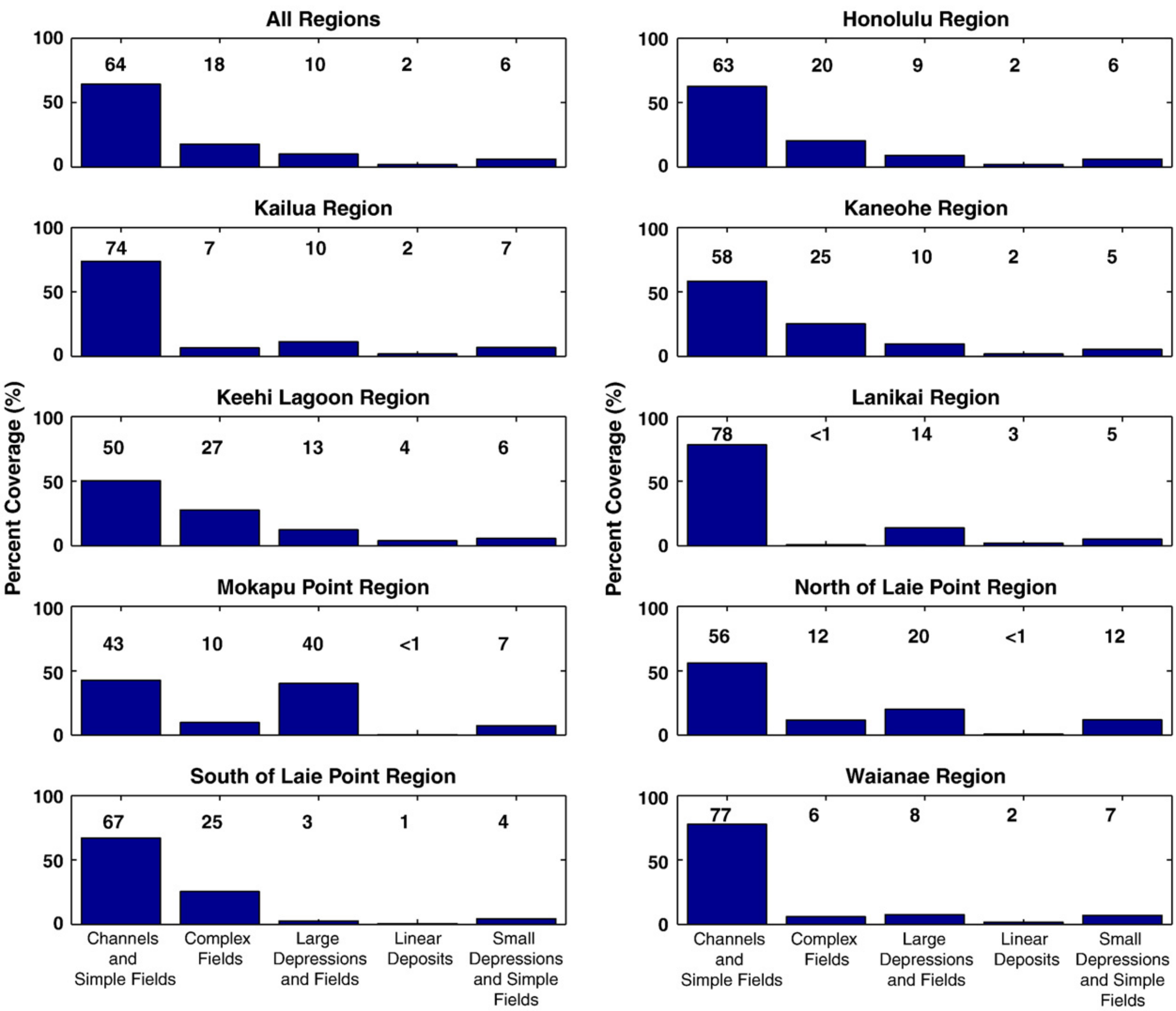

Fig. 7. Bar plots showing class distributions for the five sand deposit classes as percent coverage in the entire study area and each of the nine study regions.

extensive on the walls, it was not sufficient to close the channel. However, immediately south is a much narrower Transitional Channel being closed by modern growth. In the 10–20 m depth, where growth generally dominates modern morphology, this channel is expressed as a series of separated depressions, all connected by a winding and narrow depression in the insular shelf (paleo-channel). In the 0–10 m depth, where antecedent topography controls bathymetry, the channel is properly classified.

This example emphasizes that our classification system works where channels maintain original morphology. In the 10–20 m depth deposit morphology is controlled more by reef growth into accommodation space than the conduit's transportation of sand. The close proximity of this Transitional Channel to a Major Channel, both of which share common hydrodynamic and ecologic environments, implies that a combination of channel width and depth are needed to preserve both channel morphology and sand conduit capability.

Sand-Starved Channels are completely disrupted and no longer active conduits of sand. Several examples of Sand-Starved Channels are identified in the bathymetry. Sand-Starved Channels are blocked by lithified outcrops rather than modern growth. One example is a former channel that is bisected by an eolianite outcrop dating from MIS 5a–d (Fletcher et al., 2005). The outcrop bisects the channel and is therefore younger. Sand-Starved Channels contain limited patches of sand and provide interesting examples of sand storage response when nearshore and offshore sand deposits are not connected. Though active channels may have outcroppings of rock within channel walls, the distinction of Sand-Starved Channels is that outcrops extend across the width of the channel and are higher than channel walls.

Unchannelized Drainage is identified by analyzing local watershed and drainage patterns for evidence of small waterways related to flood drainage or wetlands during lower sea-levels. These are minor drainage systems that do not show modern evidence of permanent channels through the subaerial, porous limestone. Modern bathymetry resembles a group of interconnected, sand-filled depressions extending from the shoreline down to the offshore fields. This morphology is likely the product of karst processes acting on the carbonate bedrock of the coastal plain. Unchannelized Drainage deposits have high surface areas and are also in the sub-environment crossing 10 m.

Misclassified Deposits are classified as Channels and Connected Fields because they have large surface areas, complex shapes, and are elongate in nature. However, they do not fit the geologic definition for Channels and Connected Fields, and are considered an error class. Included in this subclassification are almost all the known, sand-filled, engineered (dredged) depressions. Engineered depressions were identified as Large Depressions and Fields for training the classifier, though their actual shapes are much closer to channels. Combined, all misclassified shapes account for only a small portion (<1%) of the overall sand deposit surface coverage. Unfortunately they have a significant effect on User's accuracy for the classification algorithm. Minor effects on total sand storage are considered negligible, even though User's accuracy is lower.

The connectivity between near- and offshore sands and the high surface area of these deposits is important. They allow sands from lower sea-levels to cross the 20 m scarp, supplying sediment to the nearshore sand budget. They store large volumes of sand, and they are production areas for modern sediment.

Sand production on Hawaii's insular shelves is associated with productivity rates of organisms such as Foraminifera, mollusks, coralline (red) algae, Echinoids, corals, and *Halimeda* (Moberly et al., 1965). Moberly et al., found Foraminifera live in sand channels and on the fore reef, but are not significantly present on the reef flat. Many other sand components, with the exception of coralline algae, are transported into the shallows from the reef edge.

Harney et al. (2000), during sediment research in Kailua Bay, found two primary sources of sediment. Offshore reef platforms are primary sources for framework sediments (coral and coralline algae) while nearshore hardgrounds and landward portions of reef platforms are sources of direct sediment production (*Halimeda*, mollusks, and Foraminifera).

Both Moberly et al. and Harney et al., agree that sediments produced on the reef platform fill spaces there, move to shallower nearshore deposits, or move off the fore reef into deeper waters. Harney et al. found that sediment production on the nearshore reef feeds sand deposits in the nearshore (including beaches) but eventually moves downslope toward offshore fields that are likely to be terminal depositional sites. These researchers and Cacchione and Tate (1998) indicate that sediments move both onshore and offshore within Major Channels, acting as a conduit system between nearshore deposits and offshore fields.

5.1.2. Complex Fields and Very Large Depressions

Fields with Steep Boundaries are generally offshore sand fields whose shoreward limits are either scarps on the insular shelf or steep sided morphologies like spur and groove. Low-energy and sediment rich areas allow offshore fields to extend shoreward into these grooves. In the low-energy Honolulu region offshore Fields with Steep Boundaries, deeper spurs help to separate sand fields from channels, so they are identified as individual. Lower annual wave energy allows for greater abundance of sub-environments >10 m depth, with extensive spur and groove development extending across the insular shelf. This, combined with the occasionally present shallow terrace, provides increased storage space for sands. Honolulu has little net accumulation of modern reef growth, as hurricanes wipe out most modern framework builders (Grigg, 1995). In addition, Waikiki shoreline in Honolulu region has received multiple sand nourishments throughout the 20th and into the 21st century, of which ~150,000 m^3 is no longer accountable on the beaches (Miller and Fletcher, 2003). Assuming this volume has moved onto the insular shelf it is enough to cover all Honolulu region's sand deposits with ~5 cm of sand.

Reefal Strandlines (Blanchon and Jones, 1995) on the shallow fringing shelf are another significant subclass of Complex Fields and Very Large Depressions with linear features parallel to the direction of wave approach across the insular shelf. Reefal Strandlines often extend straight back from the break in slope on the insular shelf to near the shoreline. Near the landward end of channels the Reefal Strandlines curve toward the channel, indicating that nearshore currents strong enough to transport sediments are being focused into the channels. Sediment production and storage along the Reefal Strandlines is linked to the beach system by wave transport and to the offshore fields by the conduit behavior of the channels. Though these features may cover large surface areas, jet probing in Waikiki, Kailua, Lanikai, and Waimanalo (Bochicchio et al., 2009) suggests that their thickness is usually minimal, indicating small volumes of sediment. Individual Reefal Strandlines often interconnect on the shallow fringing shelf, producing deposit orientations that are shore-parallel.

Radial Lineations (Guilcher, 1988) are oriented to wave approach across the reef and are shaped by wave energy as sediment is transported toward the landward margin of the shallow fringing shelf. Radial Lineations are not thick deposits, but they may adjoin sand cays and other types of sand accumulations. Three examples of Radial Lineations were identified, all in lagoon environments.

Very Large Depressions are likely the result of karst features such as dolines or uvalas developed during subaerial exposure of Oahu reefal carbonates. Dolines form as roughly circular depressions up to the size of valleys, while uvalas are typically more irregular in shape and are larger in surface area. These are complex features in shallow water with long-axes oriented in the direction of wave approach. It is most likely that these depressions became linked after marine inundation.

The difference in geologic history between Very Large Depressions and Fields with Steep Boundaries is from morphologic control due to antecedent topography rather than reef growth. This does not affect potential sand storage space as both create relatively deep and interconnected storage spaces for sands.

Open Fields appear to be located within minor depressions in the reef, and often contain many outcrops and irregular perimeters. This subclass fills in gentle bathymetric lows, or swales, and tapers out as the basin floor rises to the surrounding hard bottom. Because of the shallow nature of these depressions, many outcrops extend through the sand deposit, and the borders are often very complex. This subclass is included in Complex Fields and Very Large Depressions because of very high complexity values.

5.1.3. Large Depressions and Fields

Fields, similar to Open Fields except that individual sand deposits have less total surface area and are less complex, are less common. They also account for far less total sand coverage than Large Depressions.

Many Large Depressions are single (or only a few connected) karst derived dolines. When located near the break in slope on the insular shelf, sand deposits in this class become more elongate and oriented in the direction of wave approach. Dolines developed in subaerial porous limestone show preferred orientations parallel to major trends (Ritter et al., 2002). Sub-environments in 0–10 m depth and crossing the 10 m contour both show preferred orientation in a generally shore-normal direction, while sub-environments in 10–20 m depth show no preferred orientation. Though the Large Depressions were created by the same process of subaerial karstification, wave and tidal current energies are needed to preserve and possibly accentuate original depression shapes.

5.1.4. Linear Deposits

These sand deposits fill in linear depressions or are deposited in linear sand ridges as a result of hydrodynamic conditions. Most deposits in the Linear Deposit class are oriented in the direction of wave approach. Exceptions occur in two locations: sand deposits located along the shoreline and large offshore sand deposits, both are cropped short by limits of detection within the imagery.

Percent regional sand coverage is fairly uniform for this class, though Keehi Lagoon and Mokapu Point regions have exceptionally high and low percent coverage respectively. Keehi Lagoon's shallow shelf (0–10 m depth), high spur and groove coverage (10–20 m depth), and extensive sand fields might explain the high number of individual sand deposits. High regional sand supply and limited wave energy allow for filling of narrow and elongate reef morphology features. In higher energy systems these would either not be present or would not hold sands, as elongate features may function as hydraulic pathways in the reef. The reason for Mokapu Point's low coverage (0.28%) is probably related to the lack of a shallow fringing shelf and its high wave energy. Linear Deposits sand class has the strongest dependence on hydrodynamic conditions.

5.1.5. Small Depressions and Simple Fields

Morphologic features on the reef surface holding this class are very similar to those holding Large Depressions. Most of these deposits are in either Small Depressions filling in karst doline features or Simple Fields.

Those few sand deposits in the sub-environment crossing 10 m have a much stronger shore-normal preferred orientation than the other two sub-environments. Doline features are being closed in the deeper sub-environment, where reef growth controls available sediment storage space on the seafloor. Simple Fields in the shallower sub-environments tend to include many individual Reefal Strandlines, Radial Lineations, and bending or connected Linear Deposits. Those within the sub-environment crossing 10 m give us a focused image of small sand deposit response across the insular shelf on the 10 m contour. Strong preferred orientation at this depth indicates control by hydrodynamic conditions forcing a preferred orientation coincident with limited reef growth.

An aspect of our methodology that may affect Small Depressions and Simple Fields is that all processing is pixel-based, while all analysis is shape-based. This transition affects marginally continuous bodies by identifying them as discrete and discontinuous sections. A portion of this class is also the result of pixel resolution being too coarse for imaging thin connections, resulting in a larger sand deposit separating into individual deposits. Even though these sand deposits are called "small," the minimum size is five pixels or 28.8 m^2, and their average size is 138 m^2, so they are large enough to be considered in environmental, ecologic, geologic, or resource studies.

5.2. Insular shelf types

A first order control in sand storage is provided by the general morphology of the insular shelf. Wide and shallow shelf areas with well-defined breaks in slope have more surface area covered by sand, while deeper fringing shelf areas and lagoonal shelf faces have less percent sand coverage. A second order control is due to the hydrodynamic environment on similar reef geomorphologies. Sand storage is highest in the general morphology we call low-energy wide shelf (Table 6) located on the south shore of Oahu. The following insular shelf types: medium-energy wide, seasonal high-energy deep, medium-energy deep, and high-energy deep, have decreasing sand storage respectively (Table 6). The eastern shoreline of Oahu can be broken into three categories, those receiving more north Pacific swell (Mokapu Point and North of Laie Point regions), those receiving less north Pacific swell with wide shelves (Lanikai and South of Laie Point), and those receiving less north Pacific swell with deep shelves (Kailua and Kaneohe Bay). The single region, Waianae, on the western shoreline is a deep shelf. It has a high-energy environment in the winter months as it receives direct and refracted north Pacific swell, but a low-energy environment in the summer months as it is protected from trade wind waves. These insular shelf types and their sand deposits are illustrated in Fig. 8.

5.2.1. Low-energy wide shelf

The southern shoreline of Oahu, with a wide coastal plain, low-energy environment, wide and shallow fringing shelf, shallow break in slope, and extensive offshore sand fields is the model for high sand surface coverage on Oahu. Honolulu and Keehi Lagoon regions, covering approximately 13% of Oahu's coastline, are both south-facing sections of insular shelf offshore of the Honolulu coastal plain. The area receives wave energy primarily from Kona storm events, seasonal south Pacific swell, and occasional hurricanes. It is partially protected from trade wind waves and is shadowed from winter swell.

Table 6
Five general insular shelf types, regional environments, and sand storage characteristics.

General type: insular shelf	Hydrodynamic energy environment	Insular shelf geomorphology	Keys and storage
Low-energy wide shelf	South Pacific swell (summer) 0.3–1.8 m heights 12–20 s periods Kona storm waves (9% of year) 3–4.5 m heights 6–10 s periods	Shallow fringing shelf <0.5 km wide (wider before artificial alteration) <1–3 m deep Variable presence of distinct break in slope 0–3 m deep	Major Channels Unchannelized Drainage Fields with Steep Boundaries Open Fields Reefal Strandlines Radial Lineations Most abundant sand
Medium-energy wide shelf	Trade wind waves (90% summer, 55–65% winter) 1.2–3 m heights 4–10 s periods Refracted north Pacific swell (winter) 1.5–4.5 m heights 12–20 s periods	Shallow fringing shelf >0.5 km wide <1–3 m deep Distinct shallow break in slope 1–3 m deep	Major Channels Fields with Steep Boundaries Open Fields Reefal Strandlines Large Depressions 2nd most abundant sand
Seasonally high-energy deep shelf	Direct and refracted north Pacific swell (winter) 1.5–4.5 m heights 12–20 s periods Direct and refracted south Pacific swell (summer)m heights 0.3–1.8 12–20 s periods Kona storm waves (9% of year) 3–4.5 m heights 6–10 s periods	Fringing shelf, variable width from <0.5 km to >1 km wide, typically narrow 2–10 m deep Generally deep break in slope 3–15 m deep	Major Channels Fields with Steep Boundaries Linear Deposits Small Depressions 3rd most abundant sand
Medium-energy deep shelf	Trade wind waves (90% summer, 55–65% winter) 1.2–3 m heights 4–10 s periods Refracted north Pacific swell (winter) 1.5–4.5 m heights 12–20 s periods	Fringing shelf, variable width, generally >0.5 km 3–10 m deep Deep break in slope >8 m deep	Major Channels Transitional Channels Very Large Depressions Large Depressions 4th most abundant sand
High-energy deep shelf	Direct and refracted north Pacific swell (winter) 1.5–4.5 m heights 12–20 s periods Trade wind waves (90% summer, 55–65% winter) 1.2–3 m heights 4–10 s periods	Fringing shelf >0.5 km wide >3 m deep Deep break in slope >5 m deep	Major Channels Sand-Starved Channels Large Depressions Small Depressions Linear Deposits Least abundant sand

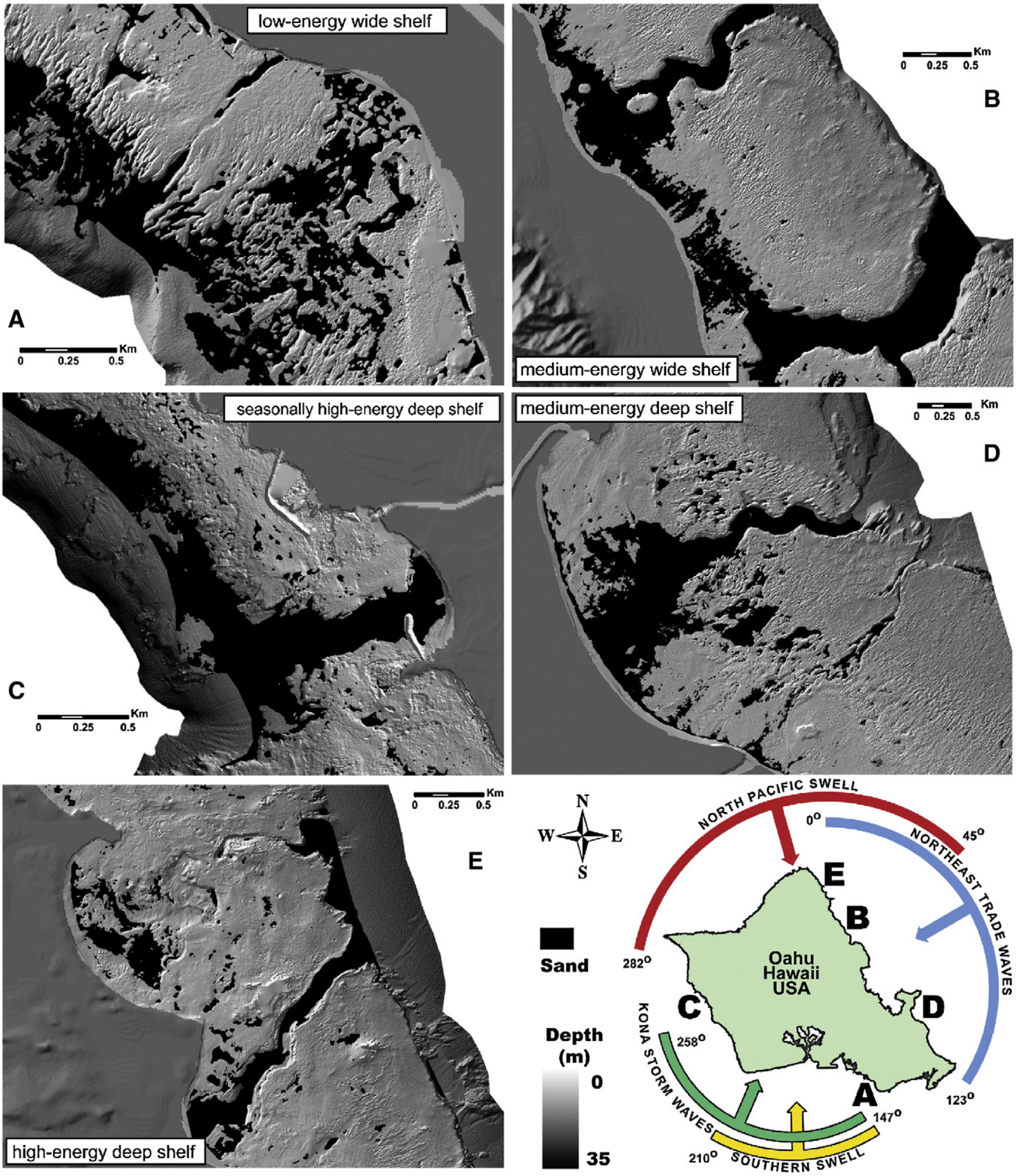

Fig. 8. Five general insular shelf types, a combination of morphology and hydrodynamic energy environment, that control sand coverage, class distribution, and sand deposit shapes. A) Low-energy wide shelf. B) Medium-energy wide shelf. C) Seasonally high-energy deep shelf. D) Medium-energy deep shelf. E) High-energy deep shelf.

High sand coverage may be the result of several factors. First, this region may have experienced increased sediment production across the wide coastal plain during the Kapapa high stand. Harney et al. (2000) documented increased sediment production on a similar coastal plain in Kailua, Oahu, during the higher sea-levels at that time. Second, damage to the southern shoreline's reefs from the 1982 and 1992 hurricanes was extensive, leaving piles of carbonate cobble and rubble where much of the living reef had formerly been (Grigg, 1995). Third, the area has been heavily dredged for channel creation and maintenance, with much of the dredge spoil dumped on the insular shelf. Fourth, high non-point source nutrient influxes might lead to increased production and consequent sediment volume increase in the area.

Relatively low wave energy from South Pacific waves combined with infrequent but catastrophic events might help to explain the abundance of carbonate sand along the southern shoreline. This does not explain the disparity in surficial coverage between Honolulu and Keehi Lagoon. These two regions also show distinct differences in sand deposit class distribution and overall sand deposit shape measurements, as seen in the glyph plots. One possible factor is the addition of sediment in the Honolulu region during beach nourishment projects, as discussed earlier. Last, both Keehi Lagoon and Honolulu regions have artificially filled coastline. The extensive loss of shallow shelf, an area of high sand cover, resulting from the development of airport runways and a manmade island has dramatically affected the Keehi Lagoon region. These three reasons are likely explanations for the disparity between percent cover in Honolulu and Keehi Lagoon regions, where the general conditions and hydrodynamic climate are otherwise very similar.

Mean sand deposit shape measurements, as seen in the regional glyphs, show that mean values for Honolulu are distinct from all other regions, and its distribution of surface coverage by classes is almost the same as the entire study area's population. Keehi Lagoon on the other hand has a sand deposit class distribution similar to Kaneohe region, the other lagoon environment, with high coverage in Complex Fields and Very Large Depressions and Linear Deposit classes and lower than average coverage in Channels and Connected Fields class. Keehi Lagoon region is similar to Lanikai in mean sand deposit shape measurements, as seen by their average glyphs, but this is probably a result of loss of shallow shelf area from dredge and filling activities. Though these regions are in different energy environments, all have broad and shallow shelves connected to well-defined and shallow breaks in slope. Lanikai and South of Laie Point regions on the eastern side of the island have similar morphologies but higher energy environments, are the next closest for percent sand coverage.

5.2.2. Medium-energy wide shelf

Lanikai and South of Laie Point regions have percent sand coverages that are similar. Both have wide, shallow shelves and very shallow and distinct breaks in slope. Mean sand deposit shape measurements, as seen in the regional glyphs, indicate that deposits in the Lanikai region are closer in shape to the deposits found at Keehi Lagoon.

5.2.3. Seasonal high-energy deep shelf

Percent sand coverage for the Waianae region is between those of morphologies with wide and shallow shelves and those with narrow and deep shelves. Though the sand deposit class distribution and morphology are similar to the Kailua region, the different energy environment allows for greater sand storage, as offshore sand fields extend into shallower depths. The offshore sand field is present in our depth of imaging around the offshore mouths of paleo-channels in the region. These offshore sand fields are positioned next to ragged scarps that are the seaward edge of a sub-environment shallower than 10 m.

Sand deposits are primarily Channels and Connected Fields class, with seven major channel systems all connected to offshore sand fields. Undulations on the insular shelf provide space for sand storage as strong long-shore currents associated with north Pacific swell move sediments along the coastline. An arid environment minimizes the presence of overly large karst depressions. However, karst features such as individual dolines or small uvalas are still present within the region. Antecedent topography is well preserved in this environment with the ragged scarp acting as the landward edge for most of the shallow offshore sand fields and is possibly inherited from previous sea-level transgressions during MIS 7and MIS 5. Arid conditions preserving several generations of karst features combined with a seasonally high-energy environment create a storage regime in Waianae that is a function of its antecedent topography. Offshore fields account for the moderately high percent of seafloor covered by sand, even with the absence of a wide fringing shelf.

5.2.4. Medium-energy deep shelf

Kailua and Kaneohe have almost identical total percent sand coverage and mean sand deposit shape measurements (glyphs). Both have prominent headlands to the north and south, both have similar preferred sand deposit orientations, comparable moderate energy environments, large and active watersheds, very limited sand storage in the 10–20 m depth zone, and offshore sand fields deeper than the limit of detection.

However, these two regions have very different morphologies. Kailua is a deep fringing shelf showing evidence of widespread karstification, dominated by a single sand channel and nearshore sand field. Kaneohe is a lagoonal environment with a broad and shallow shelf and a ramped shelf face covered in linear morphologic features on several scales. It has an active sand channel at each end, and multiple large sand fields along the landward margin. These differences are highlighted by sand deposit class distributions. Kailua is similar to the Waianae region, with a ramped shelf face and a surface dominated by sand channels. Kaneohe, on the other hand, shares many characteristics with the Keehi Lagoon region.

5.2.5. High-energy deep shelf

The high-energy environments, Mokapu Point and North of Laie Point, are both in front of wide coastal plains and have deep fringing shelves and minor sand fields that have been identified offshore. Both these regions have low total percent sand coverage, and similar mean sand deposit shape measurements (glyphs) and variations from the average for their sand deposit class distribution. Comparable morphologies, high-energy environments, and the limited watershed drainage for both of the regions explain these similarities. Higher energy waves force the deepest sub-environment into waters beyond our depth of imaging. This preserves antecedent topography, allowing for sand storage in depressions that would normally be filled or reshaped by reef growth. Lack of reef-controlled morphology reduces the presence of hydrodynamically-controlled linear features in this area. Limited watershed drainage also reduces the presence of paleo-channels within regions. This results in a restricted conduit system connecting the shallower sub-environment extending deeper than the 10 m isobath, and dominated by antecedent topography, with offshore sand fields deeper than the limit of detection.

6. Conclusions

First order control on sand storage is exerted by morphology, and second order control is provided by the level of hydrodynamic energy within the environment. In addition, almost all surface sands are located in waters less than 10 m deep and in deposits that cross the 10 m isobath. This is because the sub-environment shallower than 10 m precludes closure of depressions by modern reef growth, and conduit systems between nearshore and offshore sand deposits act as storage basins as well as conduits. These shallow areas also have the highest sediment production. The result is that the greatest sand storage is in both shelves with offshore sand fields and some wide and shallow shelves, in low-energy environments (examples are Honolulu and Keehi Lagoon). Second highest sand coverage is found on shelves without offshore fields but with extensive wide and shallow shelves, and moderately high wave energy (Lanikai, South of Laie Point). The third highest coverage is in shelves with offshore fields, but without wide and shallow shelves, in seasonally high-energy environments (Waianae). Shelves without offshore fields and wide and shallow shelves have the least sand coverage, though they can be further separated by the levels of wave energy they are exposed to: moderately high (Kailua, Kaneohe), and high (Mokapu Point, North of Laie Point).

Percent regional sand coverage is highly indicative of general morphology and annual levels of wave energy. Sand deposit class distribution and mean sand deposit shape measurements (glyphs) identify patterns associated with environmental factors. As an example, the southern shoreline of Oahu is the most sand-rich reef on Oahu. Sediment productivity rates, a function of hydrodynamic climate, ecology, and available sediment production space, are high. This is a result of exposure to refracted trade wind swell and South Pacific swell. High-energy hurricane waves and anthropogenic effects aid by providing short term, high volume increases to the sediment budget.

Sand deposit classification reveals that highest percent coverage is within the Channels and Connected Fields class. Major Channels and Unchannelized Drainage subclasses, both in the sub-environment crossing the 10 m isobath, account for almost all of this class' surface coverage. These two subclasses provide the connectivity between nearshore and offshore sand fields, acting as conduits within the insular shelf's sediment system. They link nearshore zones of sediment production with regions of sand storage.

The distinction of sand deposit classes is non-trivial. Class structures need significant numerical boundaries within shape measurements that corroborate well with physical boundaries within geologic settings. Because the data is unimodal, use of a supervised classification algorithm is necessary and numerical boundary placement is an iterative process. Regardless, sand identification through remotely sensed data is significantly faster and more accurate than hand digitizing. This process needs strict analyst control, and some hand digitization is needed to fill data gaps.

Identification of sandy marine substrate is an important component of any nearshore analysis targeting sediment resources, habitat, or substrate type. Additionally, these nearshore sands are a critical component of the littoral systems that control shoreline location on sandy coasts, as well as being highly mobile areas of the bathymetric profiles. The process of identification and characterization of sandy substrate is exportable to any coastal region, though the class structure defined in this work is most applicable to high volcanic islands with insular shelves. This process, if not the class structure itself, can be an integral first step for studies researching critical marine habitats, sediment availability and transport, and coastal erosion.

Acknowledgments

We would like to acknowledge the Office of Naval Research for providing the funding through award N00014-02-0799. We would also like to thank the U.S. Geological Survey and the U.S. Army Corps of Engineers for providing the LIDAR data, and Digital Globe for providing the QuickBird data. C.L. Conger wishes to thank Bill Morrison and Ayesha Genz for their continued support and technical expertise.

This paper is funded in part by a grant/cooperative agreement from the National Oceanic and Atmospheric Administration, Project # R/TR-6, which is sponsored by the University of Hawaii Sea Grant College Program, SOEST, under the Institutional Grant No. NA05OAR4171048 from the NOAA Office of Sea Grant, Department of Commerce. The views expressed herein are those of the author(s) and do not necessarily reflect the views of NOAA or any of its subagencies. UNIHI-SEAGRANT-JC-10-01.

References

Blanchon, P., Jones, B., 1995. Marine-plantation terraces on the shelf around Grand Cayman: a result of stepped Holocene sea-level rise. Journal of Coastal Research 11 (1), 1–33.

Bochicchio, C., Fletcher, C.H., Dyer, M., Smith, T., 2009. Reef-top sediment bodies: Windward Oahu, Hawaii. Pacific Science 63 (1), 61–82.

Bodge, K.R., Sullivan, S.P., 1999. Hawaii Pilot Beach Restoration Project: Coastal Engineering Investigation. State of Hawaii Department of Land and Natural Resources, Honolulu.

Cacchione, D.A. and Tate, G.B., 1998. Bottom currents, waves and sand transport in a reef channel off Kailua, Hawai'i, First Regional Conference on Coastal Erosion Management in Hawai'i and Other Pacific Islands, Kihei, Maui, Hawai'i.

Conger, C.L., Hochberg, E., Fletcher, C., Atkinson, M., 2006. Decorrelating remote sensing color bands from bathymetry in optically shallow waters. IEEE Transactions on Geoscience and Remote Sensing 44 (6), 1655–1660.

Finkl, C.W., 2004. Leaky valves in littoral sediment budgets: loss of nearshore sand to deep offshore zones via chutes in barrier reef systems, southeast coast of Florida, USA. Journal of Coastal Research 20 (2), 605–611.

Fletcher, C.H., Sherman, C.E., 1995. Submerged shorelines on Oahu, Hawai'i: archive of episodic transgression during the deglaciation. Journal of Coastal Research, Holocene Cycles: Climate, Sea Levels, and Sedimentation 141–152 Special Issue 17.

Fletcher, C.H., et al., 2005. Age and origin of Late Quaternary eolianite, Kaiehu Point (Moomomi), Molokai, Hawaii. Journal of Coastal Research, Special Issue 54–73.

Fletcher, C.H., Bochicchio, C., Conger, C.L., Engels, M., Feirstein, E.J., Grossman, E.E., Harney, J.N., Rooney, J.J., Sherman, C.E., Vitousek, S., Rubin, K., Murray-Wallace, C.V. (2008) Geology of Hawaii Reefs. Chapter 11 [54p] in "Coral Reefs of the U.S.A.", Springer, 550p.

Grigg, R.W., 1995. Coral reefs in an urban embayment in Hawaii: a complex case history controlled by nature and anthropogenic stress. Coral Reefs 14 (4), 253–266.

Grigg, R.W., 1998. Holocene coral reef accretion in Hawaii: a function of wave exposure and sea level history. Coral Reefs 17, 263–272.

Grigg, R.W., Epp, D., 1989. Critical depth for the survival of coral islands: effects on the Hawaiian Archipelago. Science 243 (4891), 638–641.

Grigg, R.W., et al., 2002. Drowned reefs and antecedent karst topography, Auau Channel, S.E. Hawaiian Islands. Coral Reefs 21, 73–82.

Grossman, E., Fletcher, C.H., 2004. Holocene reef development where wave energy reduces accommodation space, Kailua Bay, Windward Oahu, Hawaii, U.S.A. Journal of Sedimentary Research 74 (1), 49–63.

Grossman, E.E., Barnhardt, W.A., Hart, P., Richmond, B.M., Field, M.E., 2006. Shelf stratigraphy and influence of antecedent substrate on Holocene reef development south Oahu Hawaii. Marine Geology 226, 97–114.

Guilcher, A., 1988. Coral Reef Geomorphology. Coastal Morphology and Research. John Wiley & Sons, New York.

Hampton, M.A., Blay, C.T., Murray, C., Torresan, L.Z., Frazee, C.Z., Richmond, B.M., Fletcher, C.H., 2003. Data report geology of reef-front carbonate sediment deposits around Oahu Hawaii. US Geological Survey Open-file Report 03-441.

Harney, J., Fletcher, C.H., 2003. A budget of carbonate framework and sediment production, Kailua Bay, Oahu, Hawaii. Journal of Sedimentary Research 73 (6), 858–868.

Harney, J., Grossman, E., Richmond, B., Fletcher, C.H., 2000. Age and composition of carbonate shoreface sediments, Kailua Bay, Oahu, Hawaii. Coral Reefs 19, 141–154.

Isoun, E., Fletcher, C.H., Frazer, N., Gradie, J., 2003. Multi-spectral mapping of reef bathymetry and coral cover; Kailua Bay, Hawaii. Coral Reefs 22, 68–82.

Lyzenga, D., 1978. Passive remote sensing techniques for mapping water depth and bottom features. Applied Optics 17 (3), 379–383.

Miller, T.L., Fletcher, C., 2003. Waikiki: historical analysis of an engineered shoreline. Journal of Coastal Research 19 (4), 1026–1043.

Moberly, R., Baver, L.D., Morrison, A., 1965. Source and variation of Hawaiian littoral sand. Journal of Sedimentary Petrology 35 (3), 589–598.

Moberly, R., Campbell, J.F. and Coulbourn, W.T., 1975. Offshore and other sand resources for Oahu, Hawaii. UNIHI-SEAGRANT-TR-75-03, Sea Grant and the Hawaii Institute of Geophysics, Honolulu.

Mumby, P.J., Green, E.P., Clark, C.D., Edwards, A.J., 1998. Digital analysis of multispectral airborne imagery of coral reefs. Coral Reefs 17 (1), 59–69.

Purdy, E.G., 1974. Reef configurations: cause and effect. In: Laporte, L.F. (Ed.), Reefs in Time and Space. Special Publication 18. Society of Economic Paleontologists and Mineralogists, Tulsa, pp. 9–76.

Rencher, A., 2002. Methods of Multivariate Analysis. John Wiley & Sons, Inc., New York. 708 pp.

Ritter, D.F., Kochel, R.C., Miller, J.R., 2002. Process Geomorphology. McGraw Hill, San Francisco. 560 pp.

Rooney, J., Fletcher, C.H., Grossman, E., Engels, M., Field, M., 2004. El Nino influence on Holocene reef accretion in Hawaii. Pacific Science 58 (2), 305–324.

Sea Engineering, I., 1993. Beach Nourishment Viability Study. Sea Engineering, Inc., Waimanalo.

Sherman, C.E., Fletcher, C.H., Rubin, K.H., 1999. Marine and meteoric diagenesis of Pleistocene carbonates from a nearshore submarine terrace, Oahu, Hawaii. Journal of Sedimentary Research 69 (5), 1083–1097.

Stearns, H.T., 1970. Ages of Dunes on Oahu, Hawaii. Occasional Paper of Bernice P. Bishop Museum, 24(4): 50-72.

Stearns, H.T., 1974. Submerged shorelines and shelves in the Hawaiian Islands and a revision of some of the eustatic emerged shorelines. Geological Society of America Bulletin 85, 795–804.

Stoddart, D.R., 1969. Ecology and morphology of recent coral reefs. Biological Reviews 44, 433–498.

Storlazzi, C.D., Logan, J.B., Field, M.E., 2003. Quantitative morphology of a fringing reef tract from high-resolution laser bathymetry: Southern Molokai, Hawaii. Geologic Society of America Bulletin 115 (11), 1344–1355.

Storlazzi, C.D., Ogsten, A.S., Bothner, M.H., Field, M., Presto, M.K., 2004. Wave- and tidally-driven flow and sediment flux across a fringing coral reef: Southern Molokai, Hawaii. Continental Shelf Research 24, 1397–1419.

Storlazzi, C.D., Brown, E., Field, M., Rogers, K., Jokiel, P.L., 2005. A model for wave control on coral breakage and species distribution in the Hawaiian Islands. Coral Reefs 24, 43–55.